Object-in-place Memory Predicted by Anterolateral Entorhinal Cortex and Parahippocampal Cortex Volume in Older Adults

Lok-Kin Yeung[1*], Rosanna K. Olsen[1,2], Bryan Hong[1], Valentina Mihajlovic[1], Maria C. D'Angelo[2], Arber Kacollja[2], Jennifer D. Ryan[1,2], and Morgan D. Barense[1,2]

Abstract

■ The lateral portion of the entorhinal cortex is one of the first brain regions affected by tau pathology, an important biomarker for Alzheimer disease. Improving our understanding of this region's cognitive role may help identify better cognitive tests for early detection of Alzheimer disease. Based on its functional connections, we tested the idea that the human anterolateral entorhinal cortex (alERC) may play a role in integrating spatial information into object representations. We recently demonstrated that the volume of the alERC was related to processing the spatial relationships of the features within an object [Yeung, L. K., Olsen, R. K., Bild-Enkin, H. E. P., D'Angelo, M. C., Kacollja, A., McQuiggan, D. A., et al. Anterolateral entorhinal cortex volume predicted by altered intra-item configural processing. *Journal of Neuroscience*, *37*, 5527–5538, 2017]. In this study, we investigated whether the human alERC might also play a role in processing the spatial relationships between an object and its environment using an eye-tracking task that assessed visual fixations to a critical object within a scene. Guided by rodent work, we measured both object-in-place memory, the association of an object with a given context [Wilson, D. I., Langston, R. F., Schlesiger, M. I., Wagner, M., Watanabe, S., & Ainge, J. A. Lateral entorhinal cortex is critical for novel object-context recognition. *Hippocampus*, *23*, 352–366, 2013], and object-trace memory, the memory for the former location of objects [Tsao, A., Moser, M. B., & Moser, E. I. Traces of experience in the lateral entorhinal cortex. *Current Biology*, *23*, 399–405, 2013]. In a group of older adults with varying stages of brain atrophy and cognitive decline, we found that the volume of the alERC and the volume of the parahippocampal cortex selectively predicted object-in-place memory, but not object-trace memory. These results provide support for the notion that the alERC may integrate spatial information into object representations. ■

INTRODUCTION

Lateral portions of the entorhinal cortex are among the earliest regions to develop tau pathology, a key biomarker for Alzheimer disease (AD; Khan et al., 2014; Braak & Braak, 1991). In turn, the presence of tau pathology here is strongly related to local gray matter loss (Maass et al., 2017; Sepulcre et al., 2016). Consistent with these findings, recent work from our group showed smaller anterolateral entorhinal cortex (alERC) volumes in ostensibly healthy older adults demonstrating early signs of preclinical AD-related cognitive decline (Olsen et al., 2017). Neurodegenerative changes in AD occur years before cognitive deficits become apparent with standard neuropsychological assessments (Sperling et al., 2011). Thus, finding a subtle cognitive effect specifically related to alERC neurodegeneration could significantly improve early detection of AD. However, these efforts are limited by a lack of understanding regarding the cognitive role of human entorhinal cortex subdivisions.

In rodents and nonhuman primates, it is well established that distinct subregions of the entorhinal cortex mediate two input pathways into the hippocampus. One pathway originates in the ventral visual stream and projects to the lateral entorhinal cortex (LEC) via the perirhinal cortex (PRC; Naber, Caballero-Bleda, Jorritsma-Byham, & Witter, 1997; Suzuki & Amaral, 1994; see also Cowell, Bussey, & Saksida, 2010). The other pathway originates in the dorsal visual stream and projects to the medial entorhinal cortex (MEC) via the postrhinal/parahippocampal cortex (PHC; Moser, Kropff, & Moser, 2008; Burwell, 2000). Far less is known about the function and organization of these two pathways in humans. Recent work suggests there exists a similar functional parcellation of the human entorhinal cortex (Maass, Berron, Libby, Ranganath, & Düzel, 2015; Navarro Schröder, Haak, Zaragoza Jimenez, Beckmann, &

[1]University of Toronto, [2]Rotman Research Institute, Baycrest Health Sciences, Toronto
*Currently at Taub Institute, Columbia University Medical Center, New York, NY.

Doeller, 2015). Functional connectivity analyses reveal that the human entorhinal cortex can be divided into two parts: an anterior-lateral subregion (the alERC) that coactivates with the PRC and a posterior-medial subregion (the pmERC) that coactivates with the PHC. This suggests a functional homology between the human alERC with the rodent LEC and between the human pmERC with the rodent MEC.

The PMAT (posterior medial, anterior temporal) model proposes that the anatomical distinction of the two pathways underlies a functional distinction as well (Ritchey, Libby, & Ranganath, 2015). Under this model, the PRC–alERC pathway is critical for representing item information, and the PHC–pmERC pathway is critical for representing spatial and contextual information, with both pathways converging in the hippocampus. Functional neuroimaging data in humans support this model, with greater BOLD activity in LEC when processing the identity of a face or object and greater BOLD activity in medial entorhinal cortex (ERC) when processing the spatial location of that object (Berron et al., 2018; Reagh et al., 2018; Reagh & Yassa, 2014; Schultz, Sommer, & Peters, 2012). Concurrently, the representational–hierarchical model proposes a hierarchical organization of stimulus representations of increasing complexity moving forward in each pathway (Cowell et al., 2010). The PRC is theorized to support object-level representations, and the hippocampus sits even higher in the hierarchy, containing even more complex conjunctive representations necessary to bind information across different objects, such as the spatial or temporal relationships constituting a scene or event. As the alERC sits between the PRC and hippocampus, this model suggests it supports representations more complex than an object, but less complex than a scene.

In contrast to human fMRI studies emphasizing the distinctiveness of the two ERC pathways, some rodent studies have reported that the separation between them is not absolute. Although the majority of connections continue along their respective pathways, the rodent LEC also has some reciprocal connections with the MEC (van Strien, Cappaert, & Witter, 2009). By analogy, similar connections between the homologous human alERC and pmERC might also exist. Based on these reciprocal connections between the two pathways, we and others have speculated that the alERC might play a role in integrating spatial information from the pmERC into the object representations supported by the PRC (Connor & Knierim, 2017; Yeung et al., 2017). Two LEC rodent studies provide support for this notion. Lesions to the rodent LEC led to impairments in "object-in-place" memory (i.e., memory for the association between an object and a spatial context), but not for memory for objects or spatial contexts independently (Wilson et al., 2013). Moreover, direct recording of the rodent LEC reported the presence of "object-trace cells": Place cells that fired specifically at the locations that had previously contained a certain object (Tsao, Moser, & Moser, 2013). In humans, we recently found that alERC volume was positively related to processing the spatial relationship of features within an object (i.e., visual fixations to the configurally relevant region of an object; Yeung et al., 2017). In this study, we sought to investigate whether the human alERC might also play a broader role in processing spatial information about an object, beyond the within-object processing that we and others have observed (Berron et al., 2018; Reagh et al., 2018; Yeung et al., 2017; Reagh & Yassa, 2014; Schultz et al., 2012). In particular, we assessed whether the integrity of the alERC was related to associating an object with its spatial context, as has been observed in rodents.

Inspired by the rodent work, we leveraged an eye-tracking-based behavioral paradigm to test whether the human alERC and surrounding medial-temporal lobe (MTL) regions might also play a role in object-in-place memory (i.e., associating an object with a particular location in a particular context) and/or object-trace memory (i.e., memory for the previous location of an object; Smith & Squire, 2008; Ryan, Leung, Turk-Browne, & Hasher, 2007; Smith, Hopkins, & Squire, 2006; Ryan & Cohen, 2004a, 2004b; Ryan, Althoff, Whitlow, & Cohen, 2000). As in our previous work, we used eye-tracking-based metrics as our outcome measures, as these measures are sensitive to memory effects, which may not reach the level of conscious awareness (Ryan et al., 2000) and allowed us to more closely match our design to the aforementioned rodent studies. A group of older adult participants with varying levels of cognitive decline incidentally viewed computer-generated scenes that were either entirely novel, repeated identically from the previous viewing, or were manipulated such that a single critical object was moved. This allowed us to derive eye-tracking-based measures of object-in-place and object-trace memory based on fixations to the location currently or previously occupied by the object in the manipulated scenes, respectively. The novel scenes were used to assess global measures of novelty detection. Furthermore, we employed a recently developed manual segmentation protocol to assess the volume of the alERC (Olsen et al., 2017; Maass et al., 2015) and surrounding hippocampal subfields and MTL cortices (Olsen et al., 2013). We hypothesized that the volumes of the alERC, the PHC, the pmERC and the hippocampal subfields, which belong to the spatial/contextual processing pathway, would relate to eye-tracking-based measures of both object-in-place memory and object-trace memory.

METHODS

Participants

Thirty-two community-dwelling older adults were recruited from the community in Toronto. Data from two participants were excluded because of eye tracker failure. The remaining 30 participants had a mean age of 72.3 years

(*SD* = 5.2 years, range = 59–81 years; 23 women). Participants had previously been tested on the Montreal Cognitive Assessment (MoCA; Nasreddine et al., 2005) within the last 23 months (mean = 12.1, *SD* = 6.8, range = 2–23 months) and were selected to provide a distribution of MoCA scores (mean = 25.3, *SD* = 3.0, range = 17–30). Given that MoCA is sensitive to the presence of mild cognitive impairment, which is associated with MTL/hippocampus volume loss (Jack et al., 1997), our intention was to select for a participant group that had a good distribution of cognitive abilities and MTL/hippocampal regional volumes. These participants were the subset of an original sample of 40 participants from Olsen et al. (2017) whom we were able to recruit for this study (i.e., eight participants were lost to follow-up). The original group of 40 participants were chosen such that 20 participants had scored above the recommended MoCA cutoff score (≥26) and 20 participants had scored below the MoCA cutoff score (<25; data on these participants has previously been reported in Olsen et al. 2017; Yeung et al., 2017). Of the 30 participants whose data we report here, 14 scored above the MoCA cutoff score, and 16 scored below it. These two groups were matched for age (participants in this study: $t(28) = 1.29, p = .21, d = 0.237$) and years of education (participants in this study: $t(28) = 0.51, p = .61, d = 0.076$). Because of our efforts to match participants above and below the MoCA cutoff score in terms of demographic characteristics, MoCA and age were not correlated among the 30 participants in this study ($r = -.250, p = .13$). For the purposes of this study, we were primarily interested in how MTL volume differences related to cognitive performance, rather than how participants who scored above/below the MoCA threshold differed; thus, we treated all the participants as a single group for all subsequent analyses. Participants received a battery of neuropsychological tests to characterize their cognitive status (Table 1) in an earlier session (mean interval = 10.2 months, *SD* = 8.8 months). All participants had normal or corrected-to-normal vision (with glasses or bifocals) and were screened for color blindness, psychological or neurological disorders, brain damage (i.e., stroke or surgery), and metal implants, which would have precluded MR imaging. All participants gave informed consent. This research received ethical approvals from the Research Ethics Boards of the University of Toronto and Baycrest.

MRI Scan Parameters

High-resolution T2-weighted images were acquired in an oblique-coronal plane, perpendicular to the long axis of the hippocampus (echo time/repetition time = 68 msec/3000 msec, 20–28 slices depending on head size, 512 × 512 acquisition matrix, voxel size = 0.43 × 0.43 × 3 mm, no skip, field of view = 220 mm), on a 3T Siemens Trio scanner at the Rotman Research Institute at Baycrest (Toronto, ON). The first slice was placed anterior to the appearance of the collateral sulcus (including the temporal pole where possible), and the last slice was placed posterior to the hippocampal tail to ensure full coverage of the entire hippocampus and all of the MTL cortices included in the volumetric analyses for all participants. To confirm slice placement, a T1-weighted magnetization prepared rapid gradient echo whole-brain anatomical scan (echo time/repetition time = 2.63 msec/2000 msec, 176 slices perpendicular to the AC–PC line, 256 × 192 acquisition matrix, voxel size = 1 × 1 × 1 mm, field of view = 256 mm) was acquired immediately before the T2-weighted scan. The T1-weighted images were also used to estimate total intracranial volume for head size correction (see Volume Correction for Head Size section).

Manual Segmentation

For each participant, L. Y. manually segmented three hippocampal subfields (CA1, dentate gyrus/CA2&3, and subiculum) and four MTL cortices (alERC, pmERC, PRC, and PHC) on coronal slices of the T2-wighted structural scans (in-plane resolution: 0.43 × 0.43 mm, 3 mm between slices) using FSLview (v3.1) (Table 2). Manual segmentation followed the Olsen–Amaral–Palombo protocol (Olsen et al., 2013; Palombo et al., 2013; see also the Appendix to Yushkevich, Amaral, et al., 2015) supplemented with a modified version of the protocol provided by Maass et al. (2015) for the subdivisions of the entorhinal cortex (see Figure 1 for a visualization of the segmentation protocol). Average volumes for each manually segmented brain region are presented in Table 3, and correlations between brain region volumes are presented in Table 4.

We considered these particular regions for two reasons. First, because these regions are directly connected to the alERC (Burwell, 2000; Suzuki & Amaral, 1994), we wished to explore if any observed alERC–behavior correlations were mediated by its inputs and outputs. Second, a number of these regions have been shown to be critically important in aspects of spatial memory, including object location memory, and scene memory. PHC lesions have been shown to impair object location memory (Malkova & Mishkin, 2003; Bohbot et al., 1998), and the PHC is reliably activated when viewing scenes (Epstein, Harris, Stanley, & Kanwisher, 1999). The hippocampus has long been known to have an important role in spatial representation (e.g., O'Keefe & Dostrovsky, 1971) and is theorized to support flexible representations of spatial/temporal arrangements of objects (Eichenbaum & Cohen, 2001) that underlie its role in scene memory and perception (Lee et al., 2005). However, the question of how structural differences in hippocampal subfields might affect these cognitive roles remains to be answered. The pmERC connects the PHC to the hippocampus, and direct recording work here suggests it is important for representing locations on a screen (Killian, Jutras, & Buffalo, 2012). The PRC is involved in combining object features into a conjunctive representation (Barense

Table 1. Neuropsychological Battery Results Expressed as Means (*SD*)

Test	*All Participants (N = 32)*		*Participants Included in Data Analysis (n = 30)*	
MoCA (/30)	25.3 (2.9)	Slightly impaired	25.3 (2.9)	Slightly impaired
WMS-IV Logical Memory				
Immediate Recall Scaled Score (/20)	11.3 (2.8)	63.7%ile	11.4 (2.9)	64.2%ile
Delayed Recall Scaled Score (/20)	10.8 (2.7)	59.1%ile	10.9 (2.8)	59.3%ile
Recognition Accuracy	78.7% (17.8%)		81.8% (11.1%)	
Trails A	43.9 sec (14.1 sec)	40.9%ile	44.1 sec (14.4 sec)	40.6%ile
Trails B	98.90 sec (35.3 sec)	52.0%ile	95.5 sec (34.5 sec)	53.2%ile
Digit Span Forward Score (/16)	10.1 (2.3)	50.6%ile	10.2 (2.3)	51.9%ile
Digit Span Backward Score (/14)	6.3 (2.3)	26.9%ile	6.4 (2.3)	28.5%ile
Rey–Osterrieth Complex Figure				
Copy (/32)	26.8 (5.7)	27.9%ile	26.6 (5.8)	27.6%ile
Immediate Recall (/32)	11.7 (6.5)	37.2%ile	12.1 (6.4)	39.5%ile
Delayed Recall (/32)	10.4 (6.6)	32.6%ile	10.7 (6.7)	34.3%ile
Weschler Abbreviated Scale of Intelligence				
Vocabulary (/80)	58.4 (10.1)	63.9%ile	58.7 (10.1)	64.8%ile
Similarities (/48)	35.8 (5.2)	74.0%ile	36.0 (5.2)	74.9%ile
Matrix Reasoning (/32)	20.7 (6.8)	72.2%ile	20.6 (7.0)	71.5%ile
Block Design (/71)	28.8 (14.7)	52.9%ile	29.3 (14.9)	53.6%ile
Visual Object and Spatial Perception Battery				
Shape Detection (/20) (Cutoff score < 15)	19.1 (1.2)	Pass	19.0 (1.2)	Pass
Incomplete Letters (/20) (Cutoff score < 16)	19.2 (0.9)	Pass	19.2 (0.9)	Pass
Dot Counting (/10) (Cutoff score < 8)	9.8 (0.4)	Pass	9.8 (0.4)	Pass
Position Discrimination (/20) (Cutoff score < 18)	19.1 (1.7)	Pass	19.1 (1.7)	Pass
Number Location (/10) (Cutoff score < 7)	9.0 (1.7)	Pass	9.0 (1.7)	Pass
Cube Analysis (/10) (Cutoff score< 6)	9.4 (1.3)	Pass	9.3 (1.3)	Pass
Silhouettes (/30) (Cutoff score < 15)	19.3 (5.3)	Pass	19.2 (5.4)	Pass
Object Decision (/20) (Cutoff score < 14)	16.6 (2.0)	Pass	16.7 (2.0)	Pass
Progressive Silhouettes (/20) (Cutoff score > 15)	10.4 (3.3)	Pass	10.2 (3.2)	Pass
Subjective memory rating (Memory Functioning Questionnaire, /448)	290.6 (54.2)	Minimal subjective difficulties	291.9 (55.3)	Minimal subjective difficulties

Maximum and cutoff scores for tests are indicated in parentheses in the left column. Note that two participants did not complete the subjective memory questionnaire. WMS-IV = Wechsler Memory Scale, 4th ed.

et al., 2012); here, we are interested in how the relationships between cognitive processes and alERC volumes may be distinct from those observed with PRC volumes. Our goal is to better understand how the alERC might contribute to all of these spatial/object memory processes that have long been associated with its surrounding MTL regions and how volumetric differences in these regions in healthy older adults might affect those processes.

Intrarater and Interrater Segmentation Reliability

Intrarater reliability was established by comparing the segmentation of five randomly selected scans by the

Table 2. Interrater and Intrarater Reliability Measurements for Manual Segmentation

	Interrater: Dice		*Interrater: ICC*		*Intrarater: Dice*		*Intrarater: ICC*	
Subregion	*Left*	*Right*	*Left*	*Right*	*Left*	*Right*	*Left*	*Right*
CA1	.88	.87	.94	.95	.74	.66	.92	.91
Subiculum	.85	.84	.89	.88	.67	.66	.81	.85
DG/CA23	.91	.90	.94	.99	.75	.73	.91	.96
alERC	.86	.85	.96	.86	.72	.73	.87	.71
pmERC	.82	.80	.90	.86	.59	.64	.95	.80
PRC	.87	.89	.98	.91	.74	.76	.98	.99
PHC	.86	.84	.89	.95	.71	.77	.86	.96

Dice was computed for both intrarater and interrater agreement. ICC(3, *k*) was calculated for intrarater, and ICC(2, *k*) was computed for interrater reliability.

same rater (L. Y.) after a delay of 1–4 months. Interrater reliability was evaluated by comparing the segmentation of five randomly selected scans by a second rater (R. K. O.) to those of L. Y. Both authors were blinded to MoCA score, task performance, and the identities of participants until after manual segmentation (including interrater and intrarater reliability) was completed. Reliability was assessed using the intraclass correlation coefficient (ICC; which evaluates volume reliability; Shrout & Fleiss, 1979) and the Dice metric (which also takes spatial overlap into account; Dice, 1945), computed separately for each region in each hemisphere. ICC(3, *k*) was computed for intrarater reliability (consistency), and ICC(2, *k*) was computed for interrater reliability (agreement). Dice was derived using the formula 2 * (area of intersecting region) / (area of original segmentation + area of repeat segmentation); a Dice overlap metric of 0 represents no overlap, whereas a metric of 1 represents perfect overlap. Intrarater and interrater reliability results are shown in Table 2. These scores are comparable to reliability values reported in the literature for manual segmentation of hippocampal subfields and MTL cortices (Yushkevich, Pluta, et al., 2015; Wisse et al., 2012) and with our previous work (Olsen et al., 2013; Palombo et al., 2013).

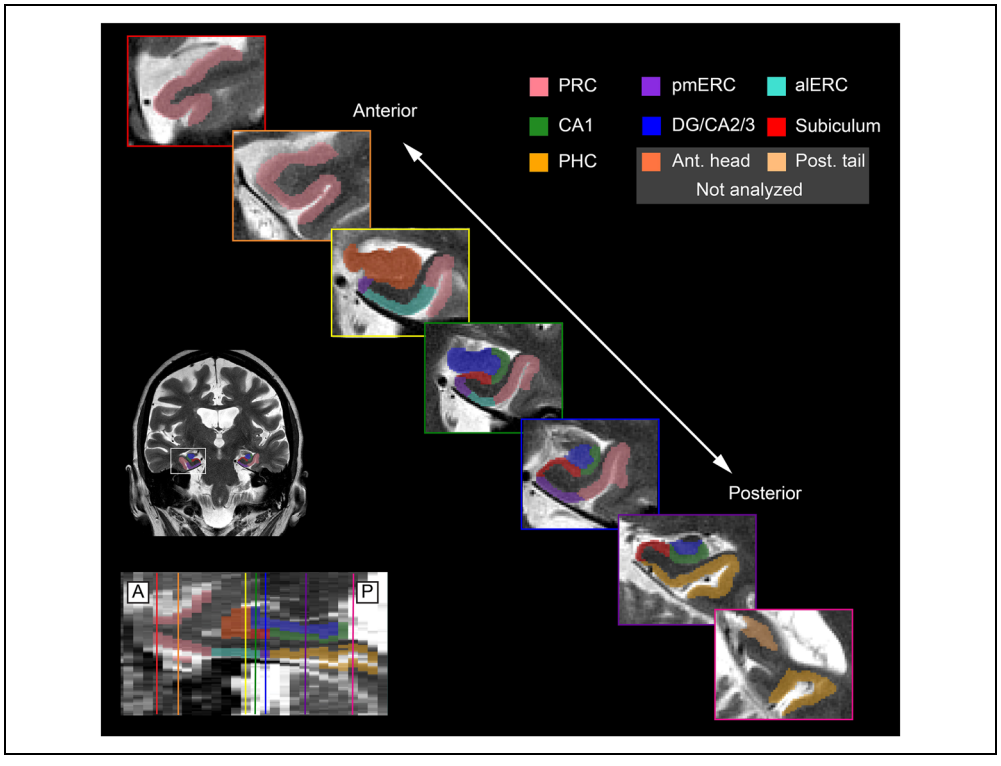

Figure 1. The modified version of the Olsen–Amaral–Palombo segmentation protocol used in this study. Inset images depict coronal slices of the MTL taken at various points along the long axis of the hippocampus (as shown in the sagittal view in figure at bottom left). Figure previously published in Olsen et al. (2017) and reproduced with permission.

Table 3. Average Volumes (±*SD*, in mm^3) for Each of the Manually Segmented Hippocampal Subfields and MTL Cortices (Corrected for Head Size)

Brain Region	*All Participants (N = 32)*	*Participants Included in Data Analysis (n = 30)*
Hippocampus		
CA1	1238.41 ± 149.33	1237.15 ± 154.22
Subiculum	1105.20 ± 192.91	1103.46 ± 194.80
DG/CA23	1957.19 ± 351.09	1963.32 ± 357.11
MTL		
PRC	4966.35 ± 1154.23	4954.03 ± 1118.44
alERC	1343.32 ± 274.72	1330.96 ± 278.97
pmERC	440.84 ± 112.80	443.50 ± 113.33
PHC	3640.21 ± 636.00	3649.43 ± 655.53

Volume Correction for Head Size

All manually segmented region volumes were corrected for head size using a regression-based method to account for differences in brain size between participants. Estimated total intracranial volume (eTIV) was derived from the whole-brain T1-weighted scans using FreeSurfer (v5.3; Buckner et al., 2004). By regressing the volume of each region with eTIV, a regression slope β was obtained for each region (representing the effect of eTIV change on that region's volume). Then, the volume of each region was adjusted by that participant's eTIV using the formula $\text{Volume}_{\text{adjusted}} = \text{Volume}_{\text{raw}} + \beta(\text{eTIV}_{\text{participant}} - \text{eTIV}_{\text{mean}})$. The head size correction was separately computed for each region in each hemisphere. In our previous work with this participant group (Olsen et al., 2017), we did not observe an interaction between cognitive decline and hemisphere. Thus, following this previous work, volumes were summed in each region across the two hemispheres, giving a single volume for each region for each participant.

Eye Tracker Setup

The experimental task was presented on a 21.2-in. monitor (36 × 30 cm) at a resolution of 1024 × 768 pixels using Experiment Builder (SR Research, Mississauga, ON). Eye-tracking measures were recorded using an EyeLink 1000 desktop-mounted eye tracker, sampling at a rate of 1000 Hz, with a spatial resolution of 0.01° and an accuracy of 0.25. Participants were positioned 55 cm away from the monitor and placed their heads on a chin-rest to limit head motion. A 9-point calibration was performed before testing and was repeated until the average gaze error was less than 1°, with no point having a gaze error exceeding 1.5°. Before each trial, a 1-sec drift correction was performed, with a 9-point calibration being repeated if drift error exceeded 2°.

Stimuli and ROIs

Eight categories of computer-generated household scenes (bathrooms, bedrooms, decks, dining rooms,

Table 4. Pearson's Correlations between Volumes of Manually Segmented Brain Regions

	CA1	*Subiculum*	*DG/CA23*	*PRC*	*alERC*	*pmERC*	*PHC*
CA1	1	.375*	.671**	.366*	.318*	.347*	.440**
Subiculum		1	.162	−.272	−.015	.590**	.228
DG/CA23			1	.468**	.258	.219	.311
PRC				1	.395*	.011	.159
alERC					1	.198	.201
pmERC						1	.274
PHC							1

*$p < .05$.

**$p < .01$.

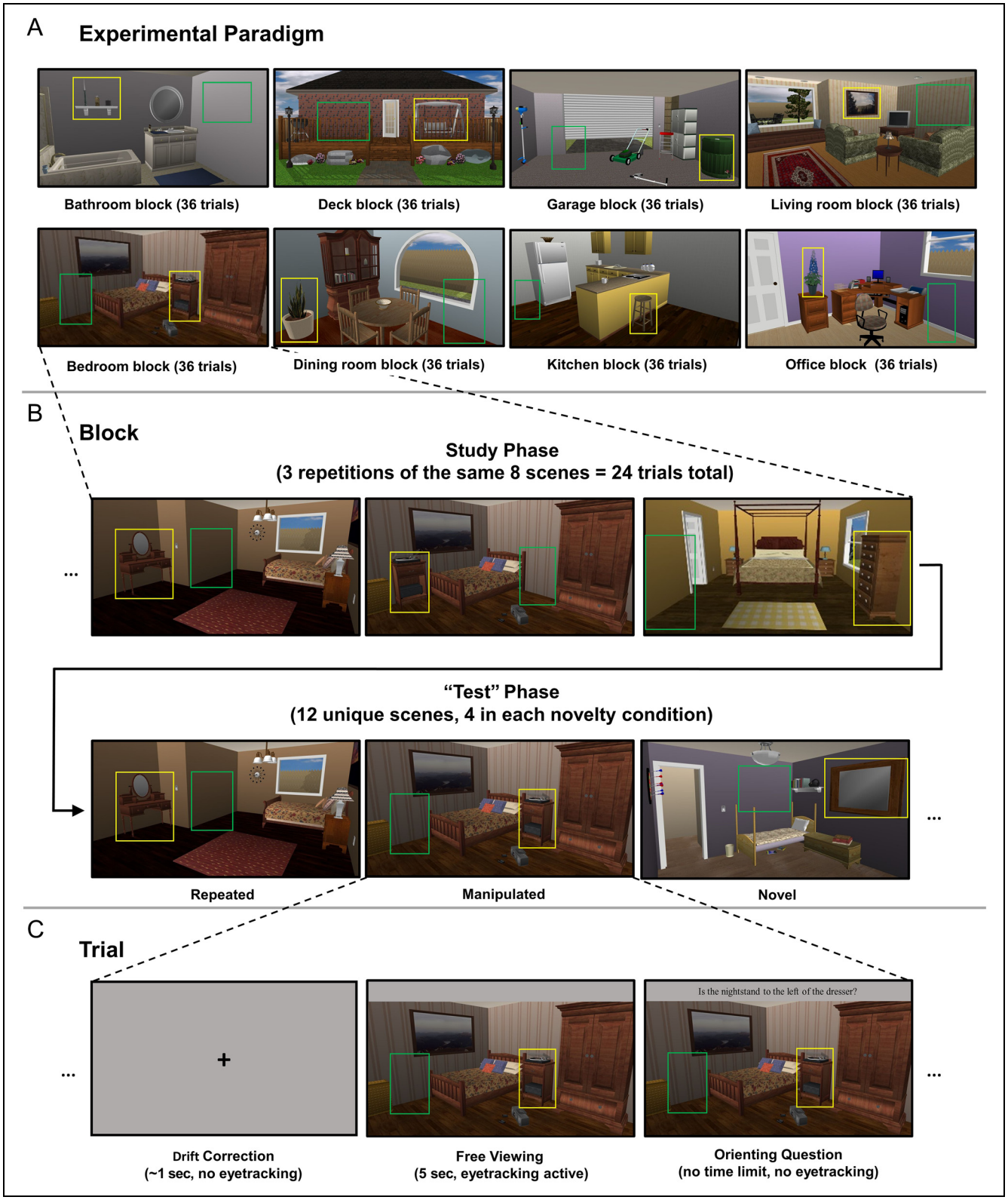

Figure 2. Schematic illustration of experimental paradigm. (A) Examples of each of the eight categories of scenes used in this study. (B) Arrangement of trials within each block. Each block had a study phase of 24 trials (eight unique scenes, repeated three times), followed by a "test" phase of 12 trials (four repeated scenes, four manipulated scenes, and four novel scenes). (C) Single trial timing. For all trials (in both study and "test" phases), after drift correction, participants freely viewed a scene for 5 sec, followed by a yes/no orienting question directed to the critical object. For illustrative purposes, in all three panels, the critical object ROI (around the critical object) is shown in yellow, and the empty ROI (a similarly sized area covering the previous location of the critical object in manipulated scenes or an empty location in repeated/novel scenes) is shown in green. Note that the ROIs were not visible to participants during the experiment.

garages, kitchens, living rooms, and offices) were used in this study (Figure 2). All stimuli were created using Punch! Home Design software (Encore Software). Each scene contained thematically appropriate objects, and all objects were unique to each individual scene. For each scene, we created two versions—a standard and an alternate. The alternate version of each scene was identical to the standard version in all respects, except for the location of a critical object within the scene. The standard version of the scene was used in all the "test" trials (i.e., it appeared in different test conditions for different participants as a result of counterbalancing). This arrangement allowed us to make direct comparisons between the same standard version of the scene, regardless of which test condition it appeared in for each individual participant. The design followed the counterbalancing procedures used in Ryan et al. (2000) and Smith et al. (2006). The standard version of each scene was also used in study trials whose scenes would be shown again in the repeated test condition. The alternate version of a scene was used for study trials whose corresponding test trial would be shown in the manipulated test condition. For instance, in Figure 2, the standard version of the scene is shown as the "test" scene in the manipulated test condition (center bottom), whereas the alternate version of the scene is shown as the corresponding study trial above it. All of the scenes measured 1028 × 518 pixels, subtending the entire width and two thirds of the height of the display screen. The scenes were centered on the screen vertically.

Three rectangular ROIs were defined for each scene (Figure 3). The "whole scene ROI" (shown in red) encompassed the entire scene depicted and was uniformly 1028 × 518 pixels large. The "critical object ROI" (shown in yellow) was drawn to include only the critical object and to minimize, as far as possible, the inclusion of parts of any other objects in the scene. The "empty ROI" (shown in green) covered an empty location in the scene and was drawn to specifically minimize, as far as possible, parts of any other objects in the scene. Importantly, the empty ROI matched the location where the critical object ROI had been located during the study phase for "manipulated" scenes (which was simply an empty location on the scene for the "repeated" and "novel" scenes). Within each scene, the critical object ROI and empty ROI were similarly, but not identically, sized. This was necessary to ensure that the ROIs did not include, as far as possible, any part of any other objects in the scene, which might receive additional fixations during the viewing period that are not directed to the critical object or the empty location. Note that no comparisons were made between the critical object ROI and the empty ROI; rather, all comparisons were within the same ROI across conditions. Across the entire stimulus set, the mean critical object ROI had an area of 36,122 pixels (6.80% of the scene, *SD* = 20,853 pixels), whereas the mean empty ROI had an area of 37,575 pixels (7.08% of the scene, *SD* = 17,778 pixels).

Eye-tracking Task

We employed an eye-tracking-based paradigm assessing processing of objects within scenes, as assessed at varying levels of novelty, and examined how volumetric differences in alERC (and other MTL/hippocampal regions) affected object-in-place memory and object-trace memory (Figures 2 and 3). In each trial, participants incidentally viewed computer-generated scenes, depicting household locations (e.g., bedrooms, kitchens), for 5 sec (Figure 2C). After viewing each scene, participants were asked to respond to a yes/no orienting question (appearing above the scene), directing attention to a critical object in the scene (e.g., "Is the nightstand to the left of the dresser?"). This followed the examples of Ryan et al. (2000) and Hannula, Tranel, and Cohen (2006), who also used orienting questions to direct viewers' attention to a

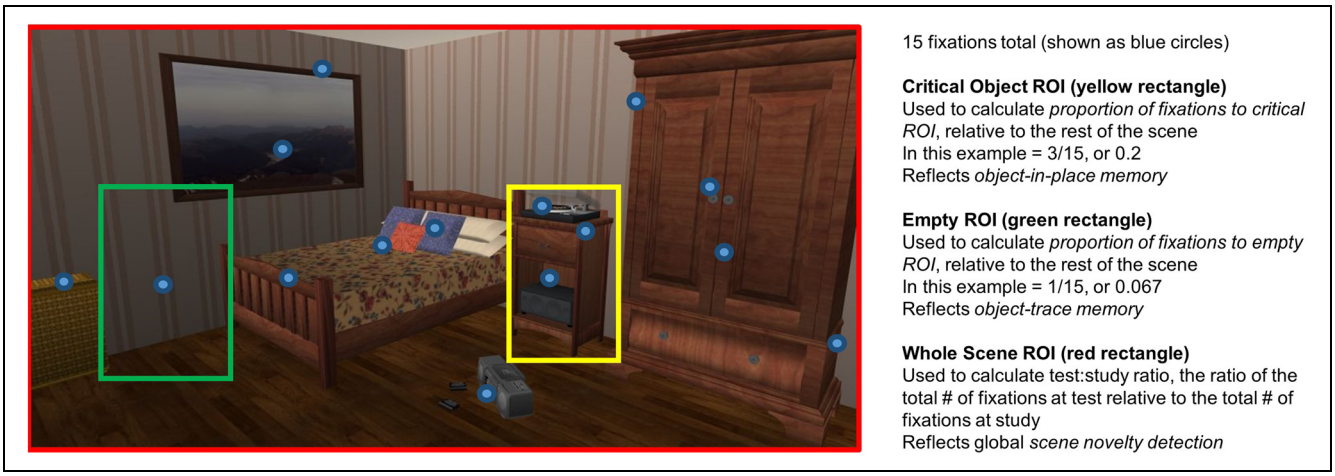

Figure 3. An example of a single manipulated scene trial, illustrating how the proportion of fixations outcome variables were calculated. Note that the ROIs and fixations were not visible to participants as they performed the task.

critical object within a scene. No time limit was imposed on answering this orienting question. Visual fixations made within the three ROIs (Figure 3) were recorded during the 5-sec viewing period, but not during the subsequent period when participants were asked to respond to the orienting question. A brief eye tracker drift correction (<1 sec) was performed between each trial.

The experiment was organized into eight blocks of 36 trials each; all the scenes in each block depicted the same type of location (e.g., one block consisted entirely of bedrooms, another block entirely of kitchens; Figure 2A). Each block included a study phase of 24 trials (eight unique scenes viewed three times each, all eight scenes were viewed at least once before any scenes repeated), followed by a "test" phase of 12 trials (Figure 2B). It is important to note that participants were not informed of any distinction between the study and "test" phases, as the task instructions were the same across all trials. In each "test" phase, there were four scenes in each of three test conditions (i.e., 12 trials total in each "test" phase), which differed in the degree of novelty (Figure 2B). The three test conditions were (1) "repeated scenes," which were identical versions of the scenes presented during the study phase; (2) "manipulated scenes," which were identical to a scene presented during the study phase, except that the critical object had moved to a different location in the scene; and (3) "novel scenes," which were not seen during the study phase but depicted the same type of scene as the rest of the block (e.g., a kitchen in a block of kitchens).

Each of the repeated or manipulated scenes shown during the "test" phase corresponded to one specific scene viewed three times during the study phase. For example, in Figure 2B, the repeated scene (bottom left) is identical to a scene viewed during the study phase (top left), whereas the manipulated scene (bottom center) is the same as the studied scene (top center), with the exception that the critical object (the nightstand) was moved from the middle of the room to the left side of the room. Furthermore, the orienting question for each specific scene (including both versions of the scenes used for the manipulated test condition) remained the same across all repetitions, as did the correct answer to that orienting question. For instance, in Figure 2, the orienting question for the middle scene (with the nightstand) was "Is the nightstand to the left of the dresser?" The answer to this question was the same ("yes") for both the alternate version of the scene shown during the study phase and the standard version of the scene shown during the "test" phase as a manipulated scene.

Across participants, the condition in which a particular scene appeared (see Stimuli and ROIs section), the ordering of the blocks, and the correct response to the orienting question for each scene were all counterbalanced. For instance, in the nightstand scene we have been using as an example, half of the participants received the alternate orienting question of "Is there a stereo on top of the nightstand?" to which the correct answer is "no" in both versions of the scene.

Eye-tracking Outcome Variables

We defined three eye-tracking-based outcome variables for each test condition based on similar measures previously employed in other studies of object-scene memory (Smith & Squire, 2008; Ryan et al., 2000, 2007; Smith et al., 2006; Ryan & Cohen, 2004a, 2004b; Figure 3). Our first primary outcome variable was the "proportion of fixations to the critical object ROI." We used this measure of viewing to assess object-in-place memory. This measure was calculated for each individual trial by dividing the number of fixations made to the critical object ROI by the total number of fixations made to the whole scene ROI and then by averaging over all the trials in a single test condition (i.e., repeated, manipulated, or novel) for each participant. In the novel scene condition, participants would not have known which object was the critical object (as they had yet to be shown the orienting question matching that scene). However, in the repeated and manipulated scene conditions, participants would have previously studied an identical (or nearly identical) version of the scene and, thus, would have had the opportunity to associate the critical object mentioned in the orienting question with its spatial location in that scene. We were particularly interested in how the proportion of fixations directed to the critical object ROI differed across the three test conditions. The difference in viewing the critical object ROI between the repeated/manipulated conditions and the novel condition reflects memory for having previously viewed the critical object. Furthermore, the difference in viewing the critical object ROI between the repeated and manipulated conditions reflects memory for the location of the critical object within that scene (i.e., object-in-place memory). We hypothesized that alERC and PHC volume would be related to this measure based on their role in object location memory. The hippocampus plays a role in spatial memory, but it remains unclear whether some or all of its subfields support this role. Our results will help elucidate which subfields support this form of spatial processing.

Our second outcome variable was the "proportion of fixations to the empty ROI" and was used to assess object-trace memory. This was calculated in a similar manner as the average proportion of fixations to the critical object ROI. For each trial, the number of fixations to the empty ROI was divided by the number of fixations to the entire scene. Then, we averaged this proportion over all the trials in each test condition separately (Figure 3). The difference in viewing between the manipulated condition and the repeated/novel conditions provided a measure of object-trace memory: Increased viewing to this otherwise-empty location reflects memory for the previous location of the critical object. By the same

rationale as above, we also hypothesized that alERC, PHC, and hippocampal subfield volumes may be related to this measure.

Our third outcome variable was the "test/study ratio." This was used to assess global scene novelty detection and to see if the differences in viewing to the critical object we observed could be explained by the broader relationship between viewing the scene as a whole and MTL regional volumes. This measure was calculated by taking the average number of fixations made to the whole scene ROIs for all the scenes in a given test condition (repeated, manipulated, or novel) and normalizing by the average number of fixations made to all the scenes during their initial presentation in the study phase. The number of fixations made to scenes during the first presentation in the study phase within each block (when all the scenes were entirely novel) served as a baseline for how many fixations a particular participant would make to an entirely novel scene. This followed the procedure we employed in our previous work (Yeung, Ryan, Cowell, & Barense, 2013) to derive a normalized eye-tracking-based measure of novelty that controlled for absolute differences in the number of fixations between participants. Because more fixations are made to novel stimuli compared with previously viewed stimuli (Althoff & Cohen, 1999), this variable served as a measure of novelty detection for the scene as a whole (i.e., scene memory). A score of 1 or more here indicates that scenes in a given test condition were being treated as novel (i.e., the same number of fixations were made as compared with when the scene was entirely novel during the first presentation of the study phase). In contrast, a score of less than 1 indicates that the scenes were visually sampled as though they had been previously seen (i.e., fewer fixations were made as compared with when the scene was entirely novel). In contrast to the previous two outcome measures, we did not predict that any MTL brain regions would be related to this measure. Because each scene is repeatedly presented from the same perspective, the novelty of the whole scene can be assessed on the basis of simple visual features (e.g., color), without reference to more complex MTL-based representations (Cowell et al., 2010). Using the scene in Figure 3 as an example to accurately remember that the nightstand is the critical object in this scene and that it was previously located at the empty location at the foot of the bed (i.e., object-in-place memory) requires us to bind those pieces of information together requiring MTL-based representations. In contrast, to identify that this scene was shown before, it is sufficient to notice simple visual features such as the stripping on the wallpaper were seen before, which does not require an MTL-based representation. This hypothesis is consistent with previous work demonstrating that amnesiac individuals with MTL damage do not show any impairments in the eye movement-based memory effect for scenes (Ryan et al., 2000). Note that this work does not imply that MTL regions are not involved in spatial processing (or that they do not perform novelty judgments in our example), merely that they are not necessary for the particular global scene novelty judgments we are investigating here.

Statistical Analysis

Repeated-measures ANOVAs and planned paired-samples t tests were used to identify differences in each of the three behavioral outcome variables (proportion of fixations to the critical object ROI, proportion of fixations to the empty ROI, test/study ratio; Figure 3) in each test condition (i.e., novel, manipulated, and repeated). Holm–Bonferroni correction was applied to the paired-samples t tests for each variable. To assess the importance of each brain region's unique contribution to the primary behavioral outcome variable, multiple regression was employed with each outcome variable as the dependent variable and the volumes of the seven brain regions as predictors for each test condition separately.

For test conditions where brain region volumes were significant predictors for a behavioral outcome variable, we were interested in whether that behavior predicted variation in brain region volume above the effects captured by existing measures of cognitive decline (e.g., the MoCA) or aging. That is, we asked: Does our outcome measure have predictive value beyond existing measures? To this end, additional multiple regression analyses were conducted with the dependent variable, MoCA, and age as predictors for the volume of those brain regions. All statistical tests were two-tailed and conducted at $\alpha = .05$. Mauchly's test of sphericity was applied to repeated-measures ANOVAs; when the assumption of sphericity was violated, the Greenhouse–Geisser correction was applied. Multiple regressions were tested for multicollinearity; residual plots were inspected to check for nonlinearity and heteroscedasticity.

RESULTS

Visual Sampling and Behavioral Responses

Orienting Question

We first looked at whether participants differed in their ability to assess the spatial relations among objects in the scene (i.e., whether they were able to accurately answer the orienting question). A repeated-measures ANOVA showed no effect of Test condition (repeated, manipulated, novel) on the accuracy of responses to the orienting question, $F(2, 58) = 0.581$, $p = .563$, $\eta^2 = .020$. Indeed, accuracy to the orienting question was uniformly high across all three test conditions: mean = 92.0%, SD = 8.1% for the repeated condition; mean = 90.5%, SD = 7.2% for the manipulated condition; and mean = 91.8%, SD = 7.0% for the novel condition. That is, across all test conditions, participants did not differ in their ability to perceptually assess spatial relations among presented objects in a scene.

Object-in-Place Memory

To investigate object-in-place memory, we ran a repeated-measures ANOVA investigating the effect of test condition (repeated, manipulated, novel) for the proportion of fixations directed to the critical object ROI. These showed a main effect of Test condition for the proportion of fixations directed to the critical object ROI, $F(2, 58) = 13.874$, $p < .001$, $\eta^2 = 0324$ (Figure 4A). Next, we compared the proportion of fixations to the critical object ROI in the repeated/manipulated scenes (where the critical object was known due to previous viewings of the scene during the study phase) to the same measure in the novel scenes (where the critical object is unknown as that scene was not shown in the study phase). Paired-samples t tests showed that a greater proportion of fixations were directed to the critical object ROI for repeated scenes than novel scenes, $t(29) = 2.342$, $p = .026$, $d = 0.453$, and for manipulated scenes than novel scenes, $t(29) = 6.301$, $p < .001$, $d = 1.009$. This suggests a memory effect for having previously viewed the critical object in the repeated and manipulated conditions. We further compared the proportion of fixations to the critical object ROI between the repeated and manipulated conditions to explore whether there was memory for the location of the critical object within the same scene. We found that the difference in the proportion of fixations to the critical object ROI between the repeated and manipulated conditions was significant, $t(29) = 2.583$, $p = .015$, $d = 0.431$, suggesting memory for the location of the critical object within the scene, beyond simply memory for the critical object (Figure 4A).

Object-trace Memory

To investigate object-trace memory, we ran a repeated-measures ANOVA investigating the effect of test condition (repeated, manipulated, novel) for the proportion of fixations directed to the empty ROI. These showed a main effect of Test condition, $F(2, 58) = 6.410$, $p = .003$, $\eta^2 = .181$ (Figure 4B). We evaluated object-trace memory across different test conditions by comparing the proportion of fixations to the empty ROI in the manipulated scenes (where the critical object had been located during the study phase) to the repeated/novel scenes (where it was only an empty location in the scene). Paired-samples t tests showed that a greater proportion of fixations were directed to the empty ROI in the manipulated condition compared with either the repeated condition, $t(29) = 2.912$, $p = .007$, $d = 0.592$, or the novel condition, $t(29) = 3.760$, $p < .001$, $d = 0.881$. In contrast, there was no difference between the repeated and novel conditions,

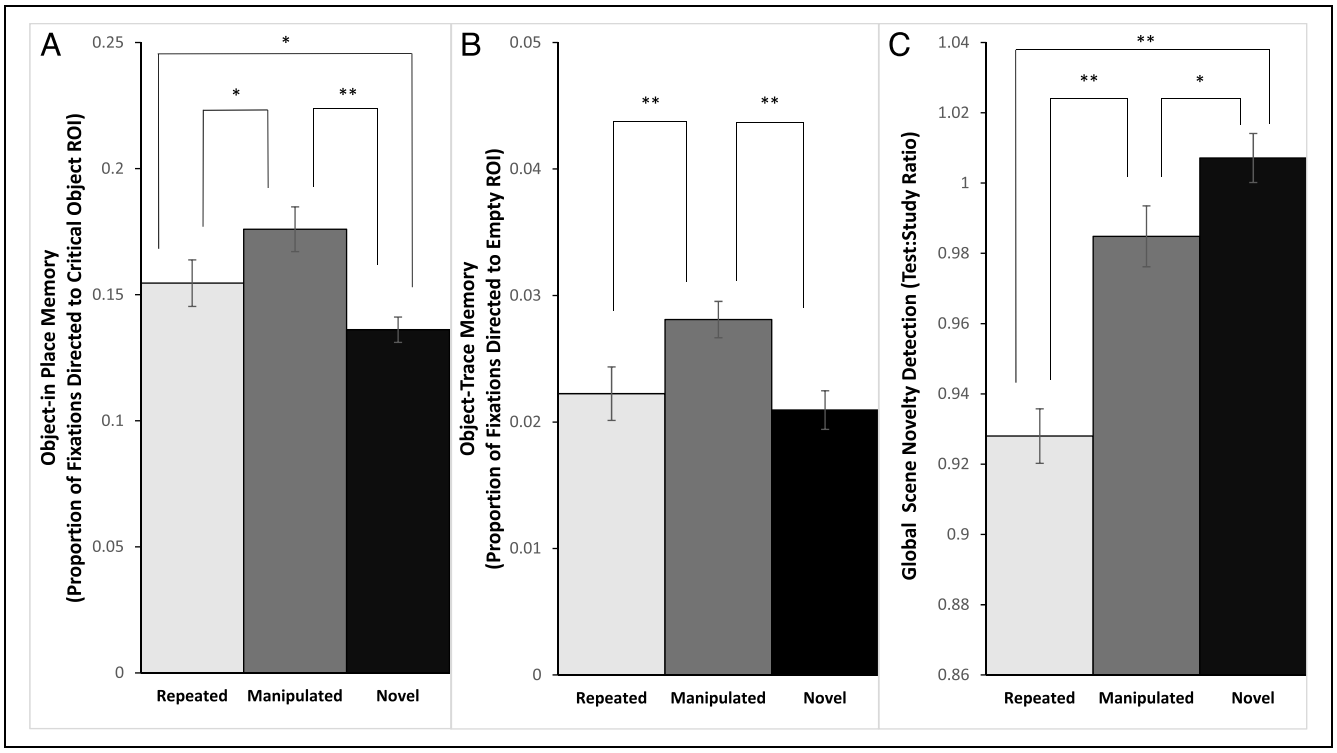

Figure 4. Behavioral eye-tracking results. (A) The proportion of fixations directed to the critical object ROI relative to the entire scene, a measure of object-in-place memory. (B) The proportion of fixations directed to the empty ROI relative to the entire scene, a measure of object-trace memory. (C) The test/study ratio, a measure of global scene novelty detection. $^{**}p < .01$, $^{*}p < .05$. Error bars represent *SEM*. $n = 30$ for all conditions.

$t(29) = 0.535$, $p = .597$, $d = 0.128$ (Figure 4B). The greater degree of viewing to the empty ROI in the manipulated scenes suggests the presence of object-trace memory for the location where the critical object was previously located.

Global Scene Novelty Detection

To investigate global scene novelty detection, we ran a third repeated-measures ANOVA investigating the effect of test condition (repeated, manipulated, novel) on the test/study ratio. These showed a main effect of Test condition for the test/study ratio (Figure 4C), $F(2, 58) = 36.786$, $p < .001$, $\eta^2 = .559$. Paired-samples t tests showed that the test/study ratio was significantly reduced (relative to novel scenes) for repeated scenes, $t(29) = 8.199$, $p < .001$, $d = 1.959$, and for manipulated scenes, $t(29) = 2.537$, $p = .017$, $d = 0.517$. Additionally, the test/study ratio was significantly reduced for the repeated scenes compared with the manipulated scenes, $t(29) = 5.649$, $p < .001$, $d = 1.263$. These results indicate a larger eye-movement based memory effect for the repeated scenes (as they received fewer fixations than the novel condition) and a smaller effect for the manipulated scenes. This replicates the eye movement-based memory effect for scenes (e.g., Ryan et al., 2000), as well as for objects (Yeung et al., 2013, 2017) as observed in our previous work.

Comparison of Healthy Versus At-risk Participants

We performed post hoc analyses, splitting our participant group on the basis of the MoCA cutoff score into "healthy" (MoCA ≥ 26, $n = 14$) and "at-risk" (MoCA < 26, $n = 16$) participants, to test if these two participant groups performed differently on any of the eye-tracking outcome measures. With the caveat that statistical power is reduced because of smaller group sizes in these analyses, we found that individual-samples t tests did not show any significant differences between these two groups for any of the three outcome measures for any of the three test conditions. Comparisons across test conditions for all three outcome measures were largely similar for both the "healthy" and "at-risk" group, with one notable exception. For global scene novelty detection, at-risk participants did not show any differences in viewing between the repeated and manipulated scenes, $t(15) = 0.748$, $p = .466$, $d = 0.206$, but healthy participants did, $t(13) = 3.372$, $p = .005$, $d = 1.344$ (i.e., there is a memory effect in the healthy, driven by a lower test/study ratio for repeated scenes vs. the at-risk participants). This echoes and extends a similar memory effect we previously found in passive viewing of highly similar lure objects (corresponding to the manipulated scenes) versus repeated objects (corresponding to the repeated scenes; Yeung et al., 2013).

Relationship between Viewing Measures and MTL Regional Volumes

Object-in-Place Memory

Next, we examined the influence of differences in MTL/hippocampal subregion volumes on viewing to the critical object ROI for each condition, our measure of object-in-place memory. Multiple regression analysis using the seven brain region volumes as predictors (Table 5A) revealed that only alERC and PHC volumes were significant predictors for the proportion of fixations made to the critical object ROI and only for the manipulated condition (alERC: $t(29) = 2.61$, $p = .02$, $\beta = 0.46$, sr = .41; PHC: $t(29) = 2.50$, $p = .02$, $\beta = 0.48$, sr = .39, statistical tests for all predictors shown in Table 5A). That is, greater alERC and PHC volume predicted a greater proportion of fixations to the critical object, but only when the critical object was moved from its position in a previously studied scene. Figure 5 illustrates this relationship graphically, plotting the unique contribution of the alERC and PHC volume predictors in the multiple regression model (i.e., alERC/PHC volume with the contributions of the other brain regions regressed out) against the proportion of fixations to the critical object. This suggests that the volumes of these two regions were related to the strength of the memory for the critical object and its spatial location within the scene.

Object-trace Memory

Next, we investigated the effect of our MTL regional volumes on viewing to the empty ROI for each condition, our measure of object-trace memory. None of the multiple regression models predicting the proportion of fixations to the empty ROI were significant for any condition (Table 5B). That is to say, MTL regional volume differences did not seem to relate to object-trace memory.

Global Scene Novelty Detection

We also calculated the relationship between MTL regional volumes and global scene novelty detection, as measured by the test/study ratio. Consistent with our previous findings (Yeung et al., 2017), none of the tested regions significantly predicted the test/study ratio for any condition (Table 5C); that is, MTL volume differences did not affect eye movement based measures of novelty for the scene as a whole. Note that this is consistent with previous reports showing that, for amnesiacs, eye movement repetition effects were normal for faces (Olsen et al., 2016; Althoff et al., 1998) and scenes (Ryan et al., 2000) when procedures are akin to those used here (e.g., multiple repetitions, relatively extended viewing time per stimulus presentation).

Table 5. Summary Tables for Multiple Regression Analyses

	Repeated			*Manipulated*			*Novel*		
Predictors	β	*t*	*sr*	β	*t*	*sr*	β	*t*	*sr*
(A) Multiple regression analyses with brain region volumes as predictors for the proportion of fixations directed to the critical object ROI in each test condition									
CA_1	−.567†	−1.869	−.325	−500†	−1.847	−.287	−.439	−1.465	−.252
Subiculum	.478†	1.725	.300	.381	1.542	.240	.303	1.106	.190
DG/CA_{23}	.016	0.063	.011	−.131	−0.591	−.092	.096	0.391	.067
PRC	.321	1.420	.247	.133	0.661	.103	.336	1.502	.259
alERC	.252	1.264	.220	**.464***	**2.607**	**.405**	.420*	2.131	.367
pmERC	−.239	−0.940	−.164	.074	0.328	.051	−.163	−0.647	−.112
PHC	.460*	2.114	.368	**.484***	**2.497**	**.388**	.098	0.456	.079
	$F(7, 22) = 1.566$, $p = .198$			$F(7, 22) = 2.775$, $p = .031$			$F(7, 22) = 1.672$, $p = .168$		
	$R^2 = .333$, $R^2_{adj} = .120$			$R^2 = .469$, $R^2_{adj} = .300$			$R^2 = .347$, $R^2_{adj} = .140$		
(B) Multiple regression analyses with brain region volumes as predictors for the proportion of fixations directed to the empty ROI in each test condition									
CA_1	−.266	−0.838	−.153	.112	0.347	.064	−.140	−0.415	−.080
Subiculum	.110	0.380	.069	.171	0.580	.108	−.028	−0.091	−.018
DG/CA_{23}	.338	1.299	.237	.184	0.694	.129	.431	1.560	.302
PRC	−.372	−1.573	−.287	−.247	−1.027	−.191	−.299	−1.189	−.230
alERC	.405†	1.942	.354	.302	1.419	.263	−.062	−0.279	−.054
pmERC	−.031	−0.117	−.021	.095	0.352	.065	.027	0.096	.019
PHC	−.223	−0.981	−.179	−.307	−1.327	−.246	−.173	−0.716	−.139
	$F(7, 22) = 1.161$, $p = .364$			$F(7, 22) = 1.006$, $p = .454$			$F(7, 22) = 0.663$, $p = .700$		
	$R^2 = .270$, $R^2_{adj} = .037$			$R^2 = .242$, $R^2_{adj} = .001$			$R^2 = .174$, $R^2_{adj} = -.089$		
(C) Multiple regression analyses with brain region volumes as predictors for the test/study ratio in each test condition									
CA_1	−.354	−1.174	−.203	−.177	−0.534	−.102	−.246	−0.781	−.141
Subiculum	−.113	−0.410	−.071	.527	1.739	.331	.348	1.211	.219
DG/CA_{23}	.317	1.282	.222	−.347	−1.276	−.243	.274	1.062	.192
PRC	−.193	−0.859	−.149	.181	0.731	.139	.385	1.639	.296
alERC	−.276	−1.392	−.241	.050	0.230	.044	.083	0.403	.073
pmERC	.025	0.099	.017	−.412	−1.486	−.283	−.429	−1.629	−.295
PHC	−.146	−.673	−.117	.223	0.940	.179	−.051	−0.227	−.041
	$F(7, 22) = 1.616$, $p = .183$			$F(7, 22) = 0.801$, $p = .595$			$F(7, 22) = 1.227$, $p = .330$		
	$R^2 = .340$, $R^2_{adj} = .129$			$R^2 = .203$, $R^2_{adj} = -.050$			$R^2 = .281$, $R^2_{adj} = .052$		

Table 5. (*continued*)

	alERC			*PHC*		
Predictors	β	*t*	*sr*	β	*t*	*sr*
(D) Multiple regression analyses with MoCA, age and viewing to the critical object ROI in the manipulated condition (object-in-place memory) as predictors for alERC and PHC volume						
MoCA	**.358***	**2.148**	**.347**	.132	0.741	.127
Age	.052	0.312	.050	−.258	−1.452	−.250
Proportion of fixations to critical object ROI	**.438***	**2.711**	**.438**	.355*	2.062	.355
	$F(3, 26) = 4.115$, $p = .016$			$F(3, 26) = 2.598$, $p = .074$		
	$R^2 = .322$, $R^2_{adj} = .244$			$R^2 = .231$, $R^2_{adj} = .142$		

In all three tables, multiple regression models were run separately for trials in each test condition. Each model is shown in its own column. $^{\dagger}p < .1$, $^{*}p < .05$, $^{**}p < .01$ (reflect tests for significance of each predictor). **Boldface** indicates significant predictors in significant multiple regression models.

Predictive Effects of Viewing Compared with MoCA and Age

Having established a connection between alERC/PHC volume and viewing behavior toward the critical object ROI in the manipulated condition, we next asked whether viewing behavior predicted change in the volumes of those regions, above and beyond the effects of MoCA or age (Table 5D). This question is important to ascertain whether the viewing behavior we report might be indicative of alERC/PHC volume differences not accounted for by existing cognitive measures. Even with MoCA and age as predictors in the same model (i.e., having accounted for the variance in alERC and PHC volume they explain), the proportion of fixations to the critical object ROI in the manipulated condition was a significant predictor for alERC volume, $t(29) = 2.71$, $p = .01$, $\beta = 0.44$, sr = .44. That is to say, the proportion of fixations to the critical object ROI for manipulated scenes explained a significant variance in alERC volume even after having accounted for the effects of cognitive decline (as assessed by the MoCA). In contrast, the multiple regression model predicting PHC volume using the same predictors only trended toward significance, $F(3, 26) = 2.60$, $p = .074$; thus, caution is to be taken in drawing strong conclusions here regarding the effects of individual predictors.

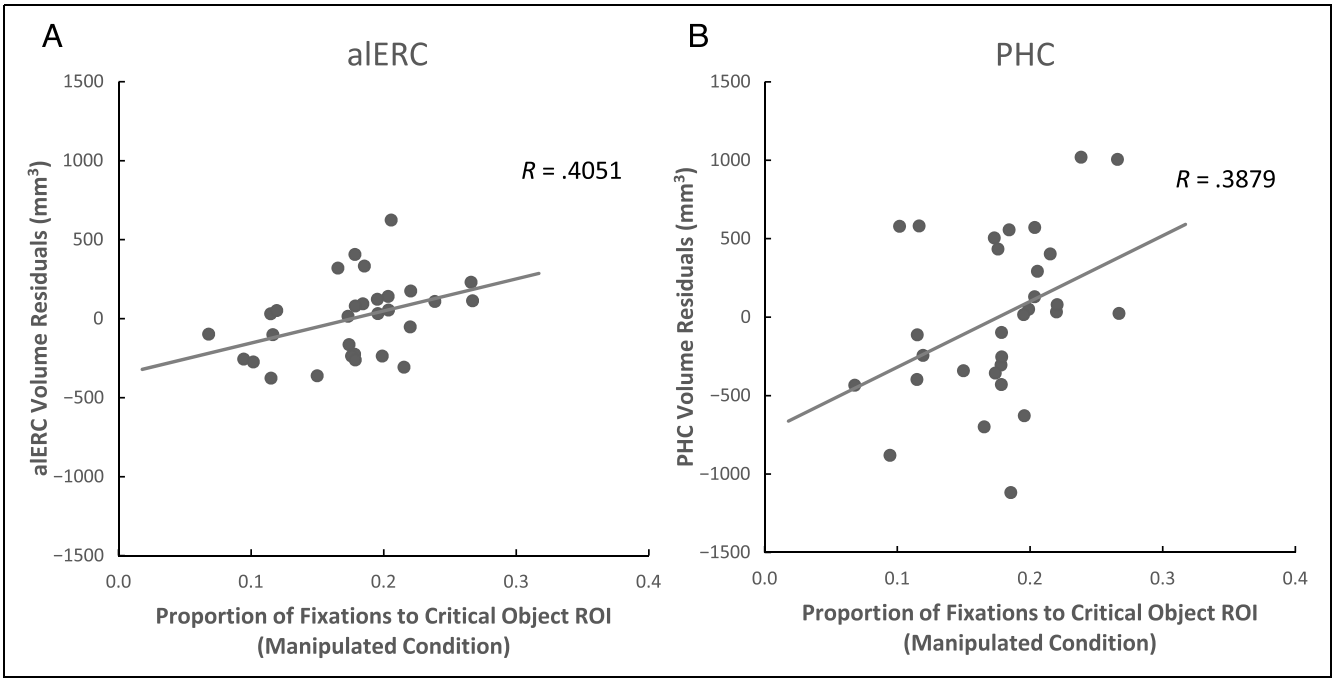

Figure 5. Correlation plots of the proportion of fixations to the critical region ROI in manipulated scenes relative to the (A) alERC residuals and (B) PHC residuals. These depict solely the contribution of the alERC and PHC predictors in Table 5A (i.e., with the contribution of other regions removed), demonstrating a correlation of alERC and PHC structural volumes with an eye movement-based measure of object-in-place processing.

DISCUSSION

The alERC is an important region in the early progression of dementia: It is coterminous with regions where AD-related tau pathology first appears in the MTL (Khan et al., 2014; Braak & Braak, 1991), and its volume is reduced in individuals who score below threshold on a neuropsychological test sensitive to AD-related cognitive decline (Olsen et al., 2017). Despite the clinical importance of the alERC, the human alERC has only recently been identified as a distinct region of the ERC, and only a few studies have looked specifically at its role in cognition. In this study, we investigated how alERC volume differences in older adults related to visual processing of objects in scenes. We found that alERC volume predicted object-in-place memory (the association of an object with a particular location in a scene). In particular, alERC volume tracked viewing to a critical object associated with a scene only when that object had moved to a new location. This is the first human study to suggest that the alERC plays a role in supporting the spatial associations of an object within a scene. It also demonstrates a remarkably specific link between brain structure and cognitive behavior: Differences in alERC volume are connected to how people direct their gaze when viewing a scene.

The PMAT model proposes that the alERC (combined with the PRC from where it receives most of its inputs) is part of a system that represents the properties of unique entities (i.e., objects). In contrast, the pmERC belongs to a different system representing the spatial, temporal, or causal relationships between entities (Ritchey et al., 2015). Previous human neuroimaging studies support this model, showing that lateral regions of the ERC are more active when differentiating between objects that differed in their features versus objects that differed by location (Reagh et al., 2018; Reagh & Yassa, 2014) and when differentiating between faces/objects compared with scenes (Berron et al., 2018; Schultz et al., 2012). This distinction is also supported by rodent studies as well (Hunsaker, Chen, Tran, & Kesner, 2013; Deshmukh, Johnson, & Knierim, 2012; Deshmukh & Knierim, 2011). In contrast to this model, some researchers have argued that the LEC also represents the spatial location of objects (Connor & Knierim, 2017; Knierim, Neunuebel, & Deshmukh, 2013). Studies have shown that rodent LEC lesions impair spatial navigation (Kuruvilla & Ainge, 2017; Van Cauter et al., 2013) and object-context memory (Wilson et al., 2013). Direct recording from rodent LEC show neurons with place fields for locations that previously held objects (Tsao et al., 2013; Deshmukh & Knierim, 2011) and neurons that are responsive to object and spatial dimensions (Keene et al., 2016). Our results provide the first evidence that the human alERC (like the rodent LEC) also plays a role in supporting the spatial relations of an object within a scene, suggesting it may have a larger role than attributed to it by the PMAT model.

These data are also consistent with the notion that there is a representational hierarchy throughout the ventral visual stream that extends into the MTL (Cowell et al., 2010; Saksida & Bussey, 2010). This model proposes that moving anteriorly through the ventral visual stream, successive regions support a hierarchy of stimulus representation, such that an object's low-level features are represented in early posterior regions, whereas increasingly complex conjunctions of object features are represented in more anterior regions (Riesenhuber & Poggio, 1999; Tanaka, 1996; Desimone & Ungerleider, 1989). Recent evidence suggests that the PRC, which receives inputs from the anterior regions of the ventral visual stream, contains representations of objects as a whole (Erez, Cusack, Kendall, & Barense, 2016; Barense et al., 2012; Bussey, Saksida, & Murray, 2002). The alERC receives inputs from the PRC, and the current results suggest the alERC supports even more complex object representations integrating spatial information about how an object relates to its environment. In turn, these alERC representations can be further combined into hippocampal-dependent representations of scenes, that is, of flexible relations among objects (see Lee, Yeung, & Barense, 2012; Olsen, Moses, Riggs, & Ryan, 2012, for reviews).

How might we reconcile our results with reports that the human LEC is not involved in spatial processing? For instance, Reagh and Yassa (2014) reported only minimal BOLD activity in human LEC when trying to ascertain whether an identical object had moved slightly in a blank field. In contrast, we report that human alERC volume affects how much we fixate on an object that has moved within a particular scene. These contrasting results suggest that the alERC's role may not be directly representing the location of an object, but rather lies in representing the spatial relations of an object within a scene (or relative to other objects). Combined with our previous work showing that alERC volume predicted viewing to configurally important regions of objects (i.e., processing the spatial relations between parts of an object; Yeung et al., 2017), these results suggest the human alERC is involved in representing some spatial properties of objects. Speculatively, the alERC may be a region where distinct information from the two systems of the PMAT system begin to converge (Suzuki & Amaral, 1994).

There is a fascinating body of work looking at direct recording from the monkey ERC during free viewing of visual images, which reported cells responsive to visual exploration (Meister & Buffalo, 2018; Killian, Potter, & Buffalo, 2015; Killian et al., 2012), analogous to cells in the rodent ERC that respond selectively to ambulatory exploration. These studies suggest that visual exploration in monkeys (and by extension, humans) is analogous to physical exploration in rodents (Shen, Bezgin, Selvam, McIntosh, & Ryan, 2016; Whishaw, 2003; Ellard, 1998) in its neural representation, explaining the correspondence between object-in-place memory in the rodent LEC (Wilson et al., 2013) and the human alERC we

report. Our results align with these findings, demonstrating a unique correspondence between visual exploration behavior and alERC volume. We note however, that spatial cells in monkeys were found in medial ERC, suggesting that our results may reflect a similar, but distinct aspect of visual exploration. How these two systems interact is worthy of future study.

We also found that PHC volume was significantly related to viewing directed to the critical object in manipulated scenes. This is consistent with reports from the lesion (e.g., Malkova & Mishkin, 2003; Bohbot et al., 1998) and functional imaging literature (e.g., Buffalo, Bellgowan, & Martin, 2006; Düzel et al., 2003; Cansino, Maquet, Dolan, & Rugg, 2002; Maguire, Frith, Burgess, Donnett, & O'Keefe, 1998) showing PHC involvement in object location memory. The PHC has also shown to be activated in response to navigationally relevant (Janzen & Van Turennout, 2004) or spatially defining objects (Mullally & Maguire, 2011); our results may reflect the influence of the PHC on viewing behavior to the critical object in relation to other scene elements. Our data also suggest this PHC function may involve the alERC, potentially reflecting the combination of information from both networks of the PMAT model. In contrast, we did not observe any effect of pmERC volume on viewing behavior. This was surprising to us, given reports of monkey visual grid cells in posterior ERC (Killian et al., 2012). However, it is theorized that the rodent medial ERC is more involved in spatial navigation (Knierim et al., 2013), and our task lacks navigational demands. It is also possible that as different grid cells code for location at different scales and orientations (Killian et al., 2012), there is an intrinsic redundancy that may help the pmERC resist behavioral changes as the result of slight volume loss.

Numerous experiments have shown that hippocampal function is related to ongoing visual exploration (e.g., Liu, Shen, Olsen, & Ryan, 2017, 2018; see Hannula, Ryan, & Warren, 2017, for a review). Whereas healthy participants typically showed a relational manipulation effect of increased viewing to manipulated regions of scenes (as we also observed in this study), amnesic cases who presented with lesions to the hippocampus (and/or surrounding MTL) did not (Ryan & Cohen, 2004a; Ryan et al., 2000). Moreover, amnesic cases with hippocampal damage did not show increased viewing toward faces associated with a particular scene (Hannula, Ryan, Tranel, & Cohen, 2007) and in fact demonstrated an altered pattern of visual exploration of faces (Olsen et al., 2015). Neuroimaging studies have also shown hippocampal BOLD activity related to eye-tracking-based measures of memory. Hippocampal BOLD activity was correlated with increased fixations to faces associated with a particular scene (Hannula & Ranganath, 2009) and fixations directed to similar locations in structurally similar scenes (Ryals, Wang, Polnaszek, & Voss, 2015); in both cases, hippocampal activation was observed even when participants were unable to explicitly articulate the similarities they observed. Given these results, we expected that hippocampal subfield volumes would relate to individual differences in viewing toward the critical object in our study; however, we did not observe such a relationship in our data. This result might be accounted for by differences in methodology and population: Our study looked at the relationship between cognitive performance and regional brain volumes in relatively healthy older adults, whereas previous work looked at fMRI activity in younger adults or cognitive performance in amnesic cases with specific lesions. There are age-related differences in eye-tracking measures; for instance, increased viewing to the critical region of manipulated scenes has been consistently reported in younger adults (Ryan et al., 2000, 2007; Smith et al., 2006), whereas this is not the case for older adults (Ryan et al., 2007). Furthermore, brain lesions can lead to greater damage in white matter tracts between MTL regions than age-related volume declines and lead to qualitatively different forms of impairment (note, however, that age-related declines in the perforant pathway between the entorhinal cortex and the hippocampus may be present in our sample; see also Yassa, Muftuler, & Stark, 2010). One plausible explanation to reconcile our results with the established literature is that hippocampal processing of object-in-place memory is constrained by its inputs from (or outputs to) the alERC. In the current participant sample, reductions in alERC volume (or alERC hypoactivity in our older adult sample; see Berron et al., 2018; Reagh et al., 2018) could act as a rate-limiting step for object-in-place memory processes in the hippocampus. Alternatively, the ERC might mediate between the hippocampus and the oculomotor system, interfacing between viewing behavior and representations required for memory (Shen et al., 2016).

Our focus on how alERC volume relates to behavior was inspired by our interest in understanding how alERC cognitive processes might be affected by neurodegeneration. As one of the earliest regions affected by AD, behavioral changes related to alERC volume changes are particularly important as possible indicators of future cognitive impairment. Although the cross-sectional nature of this study does not allow us to draw conclusions about whether the differences in visual exploration behavior related to spatial processing of objects we observe is indicative of future cognition, a longitudinal follow-up of this group would answer that question. In the long-term, tasks like the one we present here, perhaps as part of a larger neuropsychological battery of region-specific cognitive tasks, might be informative of dementia-related brain changes. This would be useful both in screening for potential dementia, as well as for assessing patients in places where neuroimaging is expensive or unavailable (as such tasks could be administered remotely; see also Whitehead et al., 2018; Whitehead, Gambino, Richter, & Ryan, 2015; Freitas Pereira, Camargo, Aprahamian, &

Forlenza, 2014; Zola, Manzanares, Clopton, Lah, & Levey, 2013; Crutcher et al., 2009).

In conclusion, we showed that, in older adults, alERC volume was selectively related to viewing behavior toward a "critical object" associated with a scene, but only when the position of that object had been moved within the scene. This study informs a newly evolving understanding of the cognitive role of the alERC, suggesting it may support aspects of spatial processing of objects. Further experimental work will be necessary to elucidate the exact nature of the alERC's cognitive role; however, this work points to the potential clinical value of eye-tracking-based tests for the early detection of dementia.

Acknowledgments

This work was supported by the Canadian Natural Sciences Engineering Research Council (Discovery and Accelerator grants to M. D. B. and Canada Graduate Scholarship [Doctoral Program] to L. Y.), a Scholar Award from the James S. McDonnell Foundation to M. D. B, and the Canada Research Chairs Program to M. D. B.

Reprint requests should be sent to Lok-Kin Yeung, Taub Institute, Columbia University Medical Center, 630 West 168th Street, P&S Box 16, New York, NY 10032, or via e-mail: ly2143@cumc.columbia.edu.

REFERENCES

Althoff, R. R., & Cohen, N. J. (1999). Eye-movement-based memory effect: A reprocessing effect in face perception. *Journal of Experimental Psychology: Learning, Memory and Cognition*, *25*, 997–1010.

Althoff, R. R., Cohen, N. J., McConkie, G., Wasserman, S., Maciukenas, M., Azen, R., et al. (1998). Eye-movement based memory assessment. In W. Becker, H. Deubel, & T. Mergner (Eds.), *Current oculomotor research: Physiological and psychological aspects* (pp. 293–302). New York: Kluwer Academic/Plenum Press.

Barense, M. D., Groen, I. I., Lee, A. C., Yeung, L. K., Brady, S. M., Gregori, M., et al. (2012). Intact memory for irrelevant information impairs perception in amnesia. *Neuron*, *75*, 157–167.

Berron, D., Neumann, K., Maass, A., Schütze, H., Fliessbach, K., Kiven, V., et al. (2018). Age-related functional changes in domain-specific medial temporal lobe pathways. *Neurobiology of Aging*, *65*, 86–97.

Bohbot, V. D., Kalina, M., Stepankova, K., Spackova, N., Petrides, M., & Nadel, L. (1998). Spatial memory deficits in patients with lesions to the right hippocampus and to the right parahippocampal cortex. *Neuropsychologia*, *36*, 1217–1238.

Braak, H., & Braak, E. (1991). Neuropathological stageing of Alzheimer-related changes. *Acta Neuropathologica*, *82*, 239–259.

Buckner, R. L., Head, D., Parker, J., Fotenos, A. F., Marcus, D., Morris, J. C., et al. (2004). A unified approach for morphometric and functional data analysis in young, old, and demented adults using automated atlas-based head size normalization: Reliability and validation against manual measurement of total intracranial volume. *Neuroimage*, *23*, 724–738.

Buffalo, E. A., Bellgowan, P. S., & Martin, A. (2006). Distinct roles for medial temporal lobe structures in memory for objects and their locations. *Learning & Memory*, *13*, 638–643.

Burwell, R. D. (2000). The parahippocampal region: Corticocortical connectivity. *Annals of the New York Academy of Sciences*, *911*, 25–42.

Bussey, T. J., Saksida, L. M., & Murray, E. A. (2002). Perirhinal cortex resolves feature ambiguity in complex visual discriminations. *European Journal of Neuroscience*, *15*, 365–374.

Cansino, S., Maquet, P., Dolan, R. J., & Rugg, M. D. (2002). Brain activity underlying encoding and retrieval of source memory. *Cerebral Cortex*, *12*, 1048–1056.

Connor, C. E., & Knierim, J. J. (2017). Integration of objects and space in perception and memory. *Nature Neuroscience*, *20*, 1493–1503.

Cowell, R. A., Bussey, T. J., & Saksida, L. M. (2010). Components of recognition memory: Dissociable cognitive processes or just differences in representational complexity? *Hippocampus*, *20*, 1245–1262.

Crutcher, M. D., Calhoun-Haney, R., Manzanares, C. M., Lah, J. J., Levey, A. I., & Zola, S. M. (2009). Eye tracking during a visual paired comparison task as a predictor of early dementia. *American Journal of Alzheimer's Disease and Other Dementias*, *24*, 258–266.

Deshmukh, S. S., Johnson, J. L., & Knierim, J. J. (2012). Perirhinal cortex represents nonspatial, but not spatial, information in rats foraging in the presence of objects: Comparison with lateral entorhinal cortex. *Hippocampus*, *22*, 2045–2058.

Deshmukh, S. S., & Knierim, J. J. (2011). Representation of non-spatial and spatial information in the lateral entorhinal cortex. *Frontiers in Behavioral Neuroscience*, *5*, 69.

Desimone, R., & Ungerleider, L. G. (1989). Neural mechanisms of visual processing in monkeys. In F. Boller & J. Grafman (Eds.), *Handbook of neuropsychology* (pp. 267–299). New York: Elsevier.

Dice, L. R. (1945). Measures of the amount of ecologic association between species. *Ecology*, *26*, 297–302.

Düzel, E., Habib, R., Rotte, M., Guderian, S., Tulving, E., & Heinze, H. J. (2003). Human hippocampal and parahippocampal activity during visual associative recognition memory for spatial and nonspatial stimulus configurations. *Journal of Neuroscience*, *23*, 9439–9444.

Eichenbaum, H. B., & Cohen, N. J. (2001). *From conditioning to conscious recollection: Memory systems of the brain*. Oxford, UK: Oxford University Press.

Ellard, C. G. (1998). Comparative perspectives on multiple cortical visual systems. *Neuroscience and Biobehavioral Reviews*, *22*, 173–180.

Epstein, R., Harris, A., Stanley, D., & Kanwisher, N. (1999). The parahippocampal place area: Recognition, navigation, or encoding? *Neuron*, *23*, 115–125.

Erez, J., Cusack, R., Kendall, W., & Barense, M. D. (2016). Conjunctive coding of complex object features. *Cerebral Cortex*, *26*, 2271–2282.

Freitas Pereira, M. L., Camargo, M. V., Aprahamian, I., & Forlenza, O. V. (2014). Eye movement analysis and cognitive processing: Detecting indicators of conversion to Alzheimer's disease. *Neuropsychiatric Disease and Treatment*, *10*, 1273–1285.

Hannula, D. E., & Ranganath, C. (2009). The eyes have it: Hippocampal activity predicts expression of memory in eye movements. *Neuron*, *63*, 592–599.

Hannula, D. E., Ryan, J. D., Tranel, D., & Cohen, N. J. (2007). Rapid onset relational memory effects are evident in eye movement behavior, but not in hippocampal amnesia. *Journal of Cognitive Neuroscience*, *19*, 1690–1705.

Hannula, D. E., Ryan, J. D., & Warren, D. E. (2017). Beyond long-term declarative memory: Evaluating hippocampal contributions to unconscious memory expression, perception, and short-term retention. In D. E. Hannula & M. C. Duff (Eds.), *The hippocampus from cells to systems* (pp. 281–336). Cham, Switzerland, Springer.

Hannula, D. E., Tranel, D., & Cohen, N. J. (2006). The long and the short of it: Relational memory impairments in amnesia, even at short lags. *Journal of Neuroscience*, *26*, 8352–8359.

Hunsaker, M. R., Chen, V., Tran, G. T., & Kesner, R. P. (2013). The medial and lateral entorhinal cortex both contribute to contextual and item recognition memory: A test of the binding ofitems and context model. *Hippocampus*, *23*, 380–391.

Jack, C. R., Jr., Petersen, R. C., Xu, Y. C., Waring, S. C., O'Brien, P. C., Tangalos, E. G., et al. (1997). Medial temporal atrophy on MRI in normal aging and very mild Alzheimer's disease. *Neurology*, *15*, 1203–1214.

Janzen, G., & Van Turennout, M. (2004). Selective neural representation of objects relevant for navigation. *Nature Neuroscience*, *7*, 673–677.

Keene, C. S., Bladon, J., Mckenzie, S., Liu, C. D., O'Keefe, J., & Eichenbaum, H. (2016). Complementary functional organization of neuronal activity patterns in the perirhinal, lateral entorhinal, and medial entorhinal cortices. *Journal of Neuroscience*, *36*, 3660–3675.

Khan, U. A., Liu, L., Provenzano, F. A., Berman, D. E., Profaci, C. P., Sloan, R., et al. (2014). Molecular drivers and cortical spread of lateral entorhinal cortex dysfunction in preclinical Alzheimer's disease. *Nature Neuroscience*, *17*, 304–311.

Killian, N. J., Jutras, M. J., & Buffalo, E. A. (2012). A map of visual space in the primate entorhinal cortex. *Nature*, *491*, 761–764.

Killian, N. J., Potter, S. M., & Buffalo, E. A. (2015). Saccade direction encoding in the primate entorhinal cortex during visual exploration. *Proceedings of the National Academy of Sciences, U.S.A.*, *112*, 15743–15748.

Knierim, J. J., Neunuebel, J. P., & Deshmukh, S. S. (2013). Functional correlates of the lateral and medial entorhinal cortex: Objects, path integration and local-global reference frames. *Philosophical Transactions of the Royal Society B: Biological Sciences*, *369*, 20130369.

Kuruvilla, M. V., & Ainge, J. A. (2017). Lateral entorhinal cortex lesions impair local spatial frameworks. *Frontiers in Systems Neuroscience*, *11*, 30.

Lee, A. C., Buckley, M. J., Pegman, S. J., Spiers, H., Scahill, V. L., Gaffan, D., et al. (2005). Specialization in the medial temporal lobe for processing of objects and scenes. *Hippocampus*, *15*, 782–797.

Lee, A. C., Yeung, L. K., & Barense, M. D. (2012). The hippocampus and visual perception. *Frontiers in Human Neuroscience*, *6*, 91.

Liu, Z.-X., Shen, K., Olsen, R. K., & Ryan, J. D. (2017). Visual sampling predicts hippocampal activity. *Journal of Neuroscience*, *37*, 599–609.

Liu, Z.-X., Shen, K., Olsen, R. K., & Ryan, J. D. (2018). Age-related changes in the relationship between visual exploration and hippocampal activity. *Neuropsychologia*, *119*, 81–91.

Maass, A., Berron, D., Libby, L. A., Ranganath, C., & Düzel, E. (2015). Functional subregions of the human entorhinal cortex. *eLife*, *4*, 1–20.

Maass, A., Landau, S., Horng, A., Lockhart, S. N., La Joie, R., Rabinovici, G. D., et al. (2017). Comparison of multiple tau-PET measures as biomarkers in aging and Alzheimer's disease. *Neuroimage*, *157*, 448–463.

Maguire, E. A., Frith, C. D., Burgess, N., Donnett, J. G., & O'Keefe, J. (1998). Knowing where things are: Parahippocampal involvement in encoding object locations in virtual large-scale space. *Journal of Cognitive Neuroscience*, *10*, 61–76.

Malkova, L., & Mishkin, M. (2003). One-trial memory for object-place associations after separate lesions of hippocampus and posterior parahippocampal region in the monkey. *Journal of Neuroscience*, *23*, 1956–1965.

Meister, M. L. R., & Buffalo, E. A. (2018). Neurons in primate entorhinal cortex represent gaze position in multiple spatial reference frames. *Journal of Neuroscience*, *38*, 2430–2441.

Moser, E. I., Kropff, E., & Moser, M. B. (2008). Place cells, grid cells, and the brain's spatial representation system. *Annual Review of Neuroscience*, *31*, 69–89.

Mullally, S. L., & Maguire, E. A. (2011). A new role for the parahippocampal cortex in representing space. *Journal of Neuroscience*, *31*, 7441–7449.

Naber, P. A., Caballero-Bleda, M., Jorritsma-Byham, B., & Witter, M. P. (1997). Parallel input to the hippocampal memory system through peri- and postrhinal cortices. *NeuroReport*, *8*, 2617–2621.

Nasreddine, Z. S., Phillips, N. A., Bédirian, V., Charbonneau, S., Whitehead, V., Collin, I., et al. (2005). The Montreal Cognitive Assessment, MoCA: A brief screening tool for mild cognitive impairment. *Journal of the American Geriatrics Society*, *53*, 695–699.

Navarro Schröder, T., Haak, K. V., Zaragoza Jimenez, N. I., Beckmann, C. F., & Doeller, C. F. (2015). Functional topography of the human entorhinal cortex. *eLife*, *4*, 1–17.

O'Keefe, J., & Dostrovsky, J. (1971). The hippocampus as a spatial map: preliminary evidence from unit activity in the freely-moving rat. *Brain Research*, *34*, 171–175.

Olsen, R. K., Lee, Y., Kube, J., Rosenbaum, R. S., Grady, C. L., Moscovitch, M., et al. (2015). The role of relational binding in item memory: Evidence from face recognition in a case of developmental amnesia. *Journal of Neuroscience*, *35*, 5342–5350.

Olsen, R. K., Moses, S. N., Riggs, L., & Ryan, J. D. (2012). The hippocampus supports multiple cognitive processes through relational binding and comparison. *Frontiers in Human Neuroscience*, *6*, 146.

Olsen, R. K., Palombo, D. J., Rabin, J. S., Levine, B., Ryan, J. D., & Rosenbaum, R. S. (2013). Volumetric analysis of medial temporal lobe subregions in developmental amnesia using high-resolution magnetic resonance imaging. *Hippocampus*, *23*, 855–860.

Olsen, R. K., Sebanayagam, V., Lee, Y., Moscovitch, M., Grady, C. L., Rosenbaum, R. S., et al. (2016). The relationship between eye movements and subsequent recognition: Evidence from individual differences and amnesia. *Cortex*, *85*, 182–193.

Olsen, R. K., Yeung, L. K., Noly-Gandon, A., D'Angelo, M. C., Kacollja, A., Smith, V. M., et al. (2017). Human anterolateral entorhinal cortex volumes are associated with cognitive decline in aging prior to clinical diagnosis. *Neurobiology of Aging*, *57*, 195–205.

Palombo, D. J., Amaral, R. S., Olsen, R. K., Müller, D. J., Todd, R. M., Anderson, A. K., et al. (2013). KIBRA polymorphism is associated with individual differences in hippocampal subregions: Evidence from anatomical segmentation using high-resolution MRI. *Journal of Neuroscience*, *33*, 13088–13093.

Reagh, Z. M., Noche, J. A., Tustison, N. J., Delisle, D., Murray, E. A., & Yassa, M. A. (2018). Functional imbalance of anterolateral entorhinal cortex and hippocampal dentate/CA3 underlies age-related object pattern separation deficits. *Neuron*, *97*, 1187.e4–1198.e4.

Reagh, Z. M., & Yassa, M. A. (2014). Object and spatial mnemonic interference differentially engage lateral and medial entorhinal cortex in humans. *Proceedings of the National Academy of Sciences, U.S.A.*, *111*, E4264–E4273.
Riesenhuber, M., & Poggio, T. (1999). Hierarchical models of object recognition in cortex. *Nature Neuroscience*, *2*, 1019–1025.
Ritchey, M., Libby, L. A., & Ranganath, C. (2015). Cortico-hippocampal systems involved in memory and cognition: The PMAT framework. In *Progress in brain research* (Vol. 219, 1st ed., pp. 45–64). Elsevier.
Ryals, A. J., Wang, J. X., Polnaszek, K. L., & Voss, J. L. (2015). Hippocampal contribution to implicit configuration memory expressed via eye movements during scene exploration. *Hippocampus*, *25*, 1028–1041.
Ryan, J. D., Althoff, R. R., Whitlow, S., & Cohen, N. J. (2000). Amnesia is a deficit in relational memory. *Psychological Science*, *11*, 454–461.
Ryan, J. D., & Cohen, N. J. (2004a). Processing and short-term retention of relational information in amnesia. *Neuropsychologia*, *42*, 497–511.
Ryan, J. D., & Cohen, N. J. (2004b). The nature of change detection and online representations of scenes. *Journal of Experimental Psychology: Human Perception and Performance*, *30*, 988–1015.
Ryan, J. D., Leung, G., Turk-Browne, N. B., & Hasher, L. (2007). Assessment of age-related changes in inhibition and binding using eye movement monitoring. *Psychology and Aging*, *22*, 239–250.
Saksida, L. M., & Bussey, T. J. (2010). The representational-hierarchical view of amnesia: Translation from animal to human. *Neuropsychologia*, *48*, 2370–2384.
Schultz, H., Sommer, T., & Peters, J. (2012). Direct evidence for domain-sensitive functional subregions in human entorhinal cortex. *Journal of Neuroscience*, *32*, 4716–4723.
Sepulcre, J., Schultz, A. P., Sabuncu, M. R., Gomez-Isla, T., Chhatwal, J., Becker, A., et al. (2016). In vivo tau, amyloid, and gray matter profiles in the aging brain. *Journal of Neuroscience*, *36*, 7364–7374.
Shen, K., Bezgin, G., Selvam, R., McIntosh, A. R., & Ryan, J. D. (2016). An anatomical interface between memory and oculomotor systems. *Journal of Cognitive Neuroscience*, *28*, 1772–1783.
Shrout, P. E., & Fleiss, J. L. (1979). Intraclass correlations: Uses in assessing rater reliability. *Psychological Bulletin*, *86*, 420–428.
Smith, C. N., Hopkins, R. O., & Squire, L. R. (2006). Experience-dependent eye movements, awareness, and hippocampus-dependent memory. *Journal of Neuroscience*, *26*, 11304–11312.
Smith, C. N., & Squire, L. R. (2008). Experience-dependent eye movements reflect hippocampus-dependent (aware) memory. *Journal of Neuroscience*, *28*, 12825–12833.
Sperling, R. A., Aisen, P. S., Beckett, L. A., Bennett, D. A., Craft, S., Fagan, A. M., et al. (2011). Toward defining the preclinical stages of Alzheimer's disease: Recommendations from the National Institute on Aging-Alzheimer's Association workgroups on diagnostic guidelines for Alzheimer's disease. *Alzheimer's & Dementia*, *7*, 280–292.
Suzuki, W. A., & Amaral, D. G. (1994). Topographic organization of the reciprocal connections between the monkey entorhinal cortex and the perirhinal and parahippocampal cortices. *Journal of Neuroscience*, *14*, 1856–1877.
Tanaka, K. (1996). Inferotemporal cortex and object vision. *Annual Review of Neuroscience*, *19*, 109–139.
Tsao, A., Moser, M. B., & Moser, E. I. (2013). Traces of experience in the lateral entorhinal cortex. *Current Biology*, *23*, 399–405.
Van Cauter, T., Camon, J., Alvernhe, A., Elduayen, C., Sargolini, F., & Save, E. (2013). Distinct roles of medial and lateral entorhinal cortex in spatial cognition. *Cerebral Cortex*, *23*, 451–459.
van Strien, N. M., Cappaert, N. L. M., & Witter, M. P. (2009). The anatomy of memory: An interactive overview of the parahippocampal–hippocampal network. *Nature Reviews Neuroscience*, *10*, 272–282.
Whishaw, I. Q. (2003). Did a change in sensory control of skilled movements stimulate the evolution of the primate frontal cortex? *Behavioural Brain Research*, *146*, 31–41.
Whitehead, J. C., Gambino, S. A., Richter, J. D., & Ryan, J. D. (2015). Focus group reflections on the current and future state of cognitive assessment tools in geriatric health care. *Neuropsychiatric Disease and Treatment*, *11*, 1455–1466.
Whitehead, J. C., Li, L., McQuiggan, D. A., Gambino, S. A., Binns, M. A., & Ryan, J. D. (2018). Portable eyetracking-based assessment of memory decline. *Journal of Clinical and Experimental Neuropsychology*, *40*, 904–916.
Wilson, D. I., Langston, R. F., Schlesiger, M. I., Wagner, M., Watanabe, S., & Ainge, J. A. (2013). Lateral entorhinal cortex is critical for novel object-context recognition. *Hippocampus*, *23*, 352–366.
Wisse, L. E. M., Gerritsen, L., Zwanenburg, J. J. M., Kuijf, H. J., Luijten, P. R., Biessels, G. J., et al. (2012). Subfields of the hippocampal formation at 7 T MRI: In vivo volumetric assessment. *Neuroimage*, *61*, 1043–1049.
Yassa, M. A., Muftuler, L. T., & Stark, C. E. (2010). Ultrahigh-resolution microstructural diffusion tensor imaging reveals perforant path degradation in aged humans in vivo. *Proceedings of the National Academy of Sciences, U.S.A.*, *107*, 12687–12691.
Yeung, L. K., Olsen, R. K., Bild-Enkin, H. E. P., D'Angelo, M. C., Kacollja, A., McQuiggan, D. A., et al. (2017). Anterolateral entorhinal cortex volume predicted by altered intra-item configural processing. *Journal of Neuroscience*, *37*, 5527–5538.
Yeung, L. K., Ryan, J. D., Cowell, R. A., & Barense, M. D. (2013). Recognition memory impairments caused by false recognition of novel objects. *Journal of Experimental Psychology: General*, *142*, 1384–1397.
Yushkevich, P. A., Amaral, R. S., Augustinack, J. C., Bender, A. R., Bernstein, J. D., Boccardi, M., et al. (2015). Quantitative comparison of 21 protocols for labeling hippocampal subfields and parahippocampal subregions in in vivo MRI: Towards a harmonized segmentation protocol. *Neuroimage*, *111*, 526–541.
Yushkevich, P. A., Pluta, J. B., Wang, H., Xie, L., Ding, S. L., Gertje, E. C., et al. (2015). Automated volumetry and regional thickness analysis of hippocampal subfields and medial temporal cortical structures in mild cognitive impairment. *Human Brain Mapping*, *36*, 258–287.
Zola, S., Manzanares, C. M., Clopton, P., Lah, J. J., & Levey, A. I. (2013). A behavioral task predicts conversion to mild cognitive impairment and Alzheimer's disease. *American Journal of Alzheimer's Disease and Other Dementias*, *28*, 179–184.